



You have downloaded a document from
RE-BUŚ
repository of the University of Silesia in Katowice

Title: Theoretical constraints on masses of heavy particles in Left-Right symmetric models

Author: Joydeep Chakraborty, Janusz Gluza, Tomasz Jeliński, Tripurari Srivastava

Citation style: Chakraborty Joydeep, Gluza Janusz, Jeliński Tomasz, Srivastava Tripurari. (2016). Theoretical constraints on masses of heavy particles in Left-Right symmetric models. "Physics Letters B" (Vol. 759, [10 August] (2016), s. 361-368), doi 10.1016/j.physletb.2016.05.092



Uznanie autorstwa - Licencja ta pozwala na kopiowanie, zmienianie, rozprowadzanie, przedstawianie i wykonywanie utworu jedynie pod warunkiem oznaczenia autorstwa.



UNIwersYTET ŚLĄSKI
W KATOWICACH



Biblioteka
Uniwersytetu Śląskiego



Ministerstwo Nauki
i Szkolnictwa Wyższego



Theoretical constraints on masses of heavy particles in Left-Right symmetric models



J. Chakraborty^a, J. Gluza^{b,*}, T. Jeliński^b, T. Srivastava^a

^a Department of Physics, Indian Institute of Technology, Kanpur 208016, India

^b Institute of Physics, University of Silesia, Uniwersytecka 4, 40-007 Katowice, Poland

ARTICLE INFO

Article history:

Received 11 May 2016

Accepted 31 May 2016

Editor: A. Ringwald

Keywords:

Unitarity

Vacuum stability

FCNC

RGEs

Left-Right symmetry

ABSTRACT

Left-Right symmetric models with general $g_L \neq g_R$ gauge couplings which include bidoublet and triplet scalar multiplets are studied. Possible scalar mass spectra are outlined by imposing Tree-Unitarity, and Vacuum Stability criteria and also using the bounds on neutral scalar masses M_{HFCNC} which assure the absence of Flavour Changing Neutral Currents (FCNC). We are focusing on mass spectra relevant for the LHC analysis, i.e., the scalar masses are around TeV scale. As all non-standard heavy particle masses are related to the vacuum expectation value (VEV) of the right-handed triplet (v_R), the combined effects of relevant Higgs potential parameters and M_{HFCNC} regulate the lower limits of heavy gauge boson masses. The complete set of Renormalization Group Evolutions for all couplings are provided at the 1-loop level, including the mixing effects in the Yukawa sector. Most of the scalar couplings suffer from the Landau poles at the intermediate scale $Q \sim 10^{6.5}$ GeV, which in general coincides with violation of the Tree-Unitarity bounds.

© 2016 The Authors. Published by Elsevier B.V. This is an open access article under the CC BY license (<http://creativecommons.org/licenses/by/4.0/>). Funded by SCOAP³.

1. Introduction

After the 2012 discovery of the spin-zero boson at the LHC [1,2] we are even more convinced that the theoretical concept of the mass generation within the gauge theory is correct. The discovered particle fits well within the predictions of the Standard Model (SM) of electroweak interactions. In the SM the mass of the Higgs boson is a free parameter. This, along with (very) weak interaction of the Higgs boson were the main reasons why it took decades to fix its mass experimentally, happened to be at the 125 GeV level [1,2]. In the meantime many theoretical concepts connected with both the scalar sector of SM and perturbation techniques have been developed and understood. It has been noted that the SM Higgs boson's mass can be bounded from both ends using quantum field theoretical (QFT) techniques [3–7]. These concepts are basic and general, and can be useful also nowadays when, after the LHC discovery, we would like to know much more. For instance, what is the actual representation of the scalar multiplets and what is the shape of the scalar potential of the fundamental theory in particle physics?

A priori, the SM theory is not the end of the story, for many reasons.

One of the main theoretical constraints on the SM Higgs boson mass comes from the simple fact that its mass depends on the strength of the Higgs quartic coupling, so the mass should not exceed an upper limit above which the theory is strongly coupled and in turn the perturbative QFT is invalid. In other words, to have a consistent weakly coupled theory involving the Higgs boson, its mass must be smaller than that upper limit. This constraint of weak interactions at high energies is called the unitarity limit. In the context of SM, the upper limit of the SM Higgs boson mass must be within $\mathcal{O}(G_F^{-1/2})$ as deduced long time ago [3–7]. This limit had been computed more precisely in [6,7] as $\sqrt{8\pi\sqrt{2}/3G_F^{-1/2}} \simeq \mathcal{O}(\text{TeV})$.

This is very important to understand the weakly coupled limit of all beyond Standard Model (BSM) theories which are considered, and which are tested in present or future accelerators, notably at the LHC. The problem has been already worked out within some popular and basic models involving two Higgs doublet models (THDM) [8–14] or models involving triplet scalar multiplets [15,16]. Unitarity constraints have been considered in [17] in the context of the Minimal Left-Right Symmetric model (MLRSM) which contains an enriched Higgs sector: a bidoublet and two

* Corresponding author.

E-mail address: januszgluza@protonmail.com (J. Gluza).

triplets scalar fields [18–20]. Some basic remarks on unitarity in the scalar sector of MLRSM can be also found in the seminal work [21]. In a recent paper [22] perturbativity and mass scales of Left-Right Higgs bosons are also discussed.

In the present study we derive Tree-Unitarity (TU) constraints in MLRSM which are written in form of individual and (or) linear combinations of the quartic couplings. Thus these bounds are easily translated in terms of the physical scalar masses. We have also combined the Vacuum Stability (VS) criteria (for recent work on this subject in a general context, see [23]) and TU constraints with Flavour Changing Neutral Currents (FCNC) bounds which give an additional limit on the mass of the right-handed charged gauge boson. In addition, in the present work we have come up with a complete set of renormalization group equations (RGEs) and perform the necessary RGEs of quartic couplings.

Interestingly, the concept of Left-Right (LR) symmetry has been revived recently at the LHC in the context of dilepton [24–28], diboson [29,30] and diphoton [31–39] excesses, which might be connected with heavy particles of LR models. It is then useful to understand possible contributions to such signals coming from the scalar sector of the theory in future studies (some first results can be found in [40]) using bounds on the scalar sector of the theory. In the context of MLRSM we started such analysis in [41], taking into account interplay of the collider signals with low energy precision data. In that paper we treated Higgs boson masses practically as free parameters, not taking into account many possible theoretical constraints. Nonetheless, there we showed that correlations between the Higgs bosons and gauge bosons as well as the radiative muon decay at 1-loop level impose strong constraints on high energy LHC signals. To understand the realistic scalar spectrum of the theory, dedicated analyses have been further performed in [42–45]. In these papers the constraints from FCNC, VS along with the LHC exclusions were considered. It has been found among others that not all four charged Higgs bosons of the theory can be simultaneously light (below 1 TeV). Taking into account this limitation, we have found several benchmark points [43,44] which are within reach of the LHC future runs. For other studies of the Higgs sector of the theory, see e.g. [46–65,45].

Here, we incorporate TU constraints and further extend the analysis. We also take care of the constraints and potentially problematic structures due to Landau poles which arise from the concept of RGEs [66]. RGEs in MLRSM have been considered at the one-loop level, originally in [67]. Here, we have performed independent RG analysis after correcting some misprints in the published article, see Sec. 5 of the present work for details. In addition, we provide a complete set of 1-loop RGEs, including all couplings of the theory. It is important for two reasons: (i) to prepare a well-tested background for higher-loops analysis, and (ii) the earlier results [67] have been used repeatedly in recent studies [68,69,17] and it is better to avoid proliferation of misprints in the future.

In the SM, as the EWSB scale is determined from the observed gauge boson masses, the upper limit on the SM Higgs boson can be fixed. Similarly, if in a near future the right-handed gauge boson masses are fixed from observation then the absolute upper mass bounds of the scalars can be provided. Thus, as of now, the bounds depend on the $SU(2)_R$ breaking scale v_R . In this paper upper limits on the heaviest mass of these Higgs bosons compatible with the TU bounds are computed as functions of v_R .

2. Model: Left-Right symmetry

The model is based on the $SU(2)_L \otimes SU(2)_R \otimes U(1)_{B-L}$ Left-Right gauge symmetry (LR) [18–20]. The spontaneous symmetry breaking occurs in two steps: $SU(2)_R \otimes U(1)_{B-L} \rightarrow U(1)_Y$, and $SU(2)_L \otimes U(1)_Y \rightarrow U(1)_{em}$. To achieve this symmetry breaking we

choose a traditional spectrum of Higgs sector multiplets with a bidoublet and two triplets [20,21]

$$\phi = \begin{pmatrix} \phi_1^0 & \phi_1^+ \\ \phi_2^- & \phi_2^0 \end{pmatrix} \equiv [2, 2, 0], \quad (1)$$

$$\Delta_{L(R)} = \begin{pmatrix} \delta_{L(R)}^+/\sqrt{2} & \delta_{L(R)}^{++} \\ \delta_{L(R)}^0 & -\delta_{L(R)}^+/\sqrt{2} \end{pmatrix} \equiv [3(1), 1(3), 2], \quad (2)$$

where the quantum numbers in square brackets are given for $SU(2)_L$, $SU(2)_R$ and $U(1)_{B-L}$ groups, respectively.

The vacuum expectation values (VEVs) of the scalar fields can be recast in the following form:

$$\langle \phi \rangle = \begin{pmatrix} \kappa_1/\sqrt{2} & 0 \\ 0 & \kappa_2/\sqrt{2} \end{pmatrix}, \quad \langle \Delta_{L,R} \rangle = \begin{pmatrix} 0 & 0 \\ v_{L,R}/\sqrt{2} & 0 \end{pmatrix}. \quad (3)$$

VEVs of the right-handed triplet (Δ_R) and the bi-doublet (ϕ), propel the respective symmetry breaking: $SU(2)_R \otimes U(1)_{B-L} \rightarrow U(1)_Y$, and $SU(2)_L \otimes U(1)_Y \rightarrow U(1)_{em}$. As $v_L \ll \kappa_{1,2} \ll v_R$, we take safely $v_L = 0$.

We set the coefficients of the quartic couplings that are linear in $\Delta_{L,R}$ to be zero [70]. We also assume that the right-handed symmetry breaking scale, v_R , is much larger than the electroweak scale, $\kappa_+ \equiv \sqrt{\kappa_1^2 + \kappa_2^2}$. Thus the terms proportional to κ_+ will be neglected comparing to the terms proportional to v_R . This assumption is phenomenologically viable and supported also by the exclusion limits given by the LHC. In addition $\kappa_1 \gg \kappa_2 \simeq 0$ [70]. These relations simplify correlations among the unphysical and physical Higgs fields which are related to each other by Eq. (74) in [71].

3. Unitarity bounds

The quartic part of the scalar potential can be written in terms of the physical fields as follows:

$$V(H_{0,1,2,3}^0; A_{1,2}^0; H_{1,2}^\pm; H_{1,2}^{\pm\pm}) = \sum_{m=1,\dots,72} \Lambda_m H_i H_j H_k H_L,$$

where $H_i, H_j, H_k, H_L \in (H_{0,1,2,3}^0; A_{1,2}^0; H_{1,2}^\pm; H_{1,2}^{\pm\pm})$. To understand the unitarity constraints one needs to look at the following scattering processes [8]:

$$H_i + H_j \rightarrow H_p + H_q, \quad (4)$$

where $H_{i,j,p,q}$ are the physical Higgs fields. These scatterings can happen in two ways at the tree level through: (i) Contact terms, i.e., four point scalar couplings which are outcome of the scalar quartic potential, and (ii) Higgs–Higgs–Gauge boson couplings. We know that the Higgs–Higgs–Gauge boson couplings contain derivatives owing to their Lorentz structure, thus when they are connected with the gauge boson exchange diagrams the maximum divergences which can appear through these diagrams are logarithmic. Considering theories up to the Planck scale, we do not need to worry about the logarithmic unitarity violations [8].

One can estimate the strength of these scalar four-point contact interactions in two ways. First, consider the process in terms of the unphysical scalar fields and reconstruct all the elements in terms of the physical neutral and charged scalars. In this case a vertex factor will be a polynomial function of the couplings which can be thought of as a rotated quartic coupling basis. As the model under consideration contains many scalar field components, it would be difficult to pin down the unitarity bounds in terms of the couplings and translate them to the masses of the scalar fields. There is an alternative option which we have adopted in this paper. Instead of rotating the quartic couplings we have sorted out all possible

quartic contact terms in terms of the physical fields where the vertex factors of each coupling are linear functions of the quartic couplings. In this way we can immediately find out the unitarity bounds on the quartic couplings. This is also helpful to translate the bounds in terms of the masses of the physical scalar fields as the mass terms possess linear dependence on the quartic couplings. Thus the unitarity bounds on the scalar masses can be easily incorporated, which is our prime aim in this analysis.

Our further strategy is as follows: to invoke that the scalars are weakly coupled we must satisfy the inequality: $|\Lambda_m| < 8\pi$ [72] for the scalar quartic couplings. There are many of them, so these couplings are gathered in [73]. Let us note that this is an improvement over [8] where the unitarity bound was given as $|\Lambda_m| < 16\pi$. For the sake of analysis it is sufficient to identify the couplings with largest coefficients. For example, if coupling λ_i appears with coefficient a_1 and a_2 such that $a_1 > a_2$, then for the unitarity constraint the $a_1\lambda_i$ term is considered, the second term will respect the unitarity bound on λ_i automatically.

As all terms with quartic couplings in four-scalar scatterings must be smaller than 8π , the following constraints on the quartic couplings follow:

$$\lambda_1 < 4\pi/3, (\lambda_1 + 4\lambda_2 + 2\lambda_3) < 4\pi, \quad (5)$$

$$(\lambda_1 - 4\lambda_2 + 2\lambda_3) < 4\pi, \quad (6)$$

$$\lambda_4 < 4\pi/3, \quad (7)$$

$$\alpha_1 < 8\pi, \alpha_2 < 4\pi, (\alpha_1 + \alpha_3) < 8\pi, \quad (8)$$

$$\rho_1 < 4\pi/3, (\rho_1 + \rho_2) < 2\pi, \rho_2 < 2\sqrt{2}\pi, \quad (9)$$

$$\rho_3 < 8\pi, \rho_4 < 2\sqrt{2}\pi. \quad (10)$$

The scalar spectrum is¹:

$$M_{H_0^0}^2 = 2 \left(\lambda_1 - \frac{\alpha_1^2}{4\rho_1} \right) \kappa_+^2, \quad (11)$$

$$M_{H_1^0}^2 = \frac{1}{2} \alpha_3 v_R^2 < 4\pi v_R^2, \quad (12)$$

$$M_{H_2^0}^2 = 2\rho_1 v_R^2 < (8\pi/3) v_R^2, \quad (13)$$

$$M_{H_3^0}^2 = \frac{1}{2} (\rho_3 - 2\rho_1) v_R^2 < (4\pi v_R^2 - M_{H_2^0}^2/2), \quad (14)$$

$$M_{A_1^0}^2 = \frac{1}{2} \alpha_3 v_R^2 - 2\kappa_+^2 (2\lambda_2 - \lambda_3) < 4\pi v_R^2, \quad (15)$$

$$M_{A_2^0}^2 = \frac{1}{2} (\rho_3 - 2\rho_1) v_R^2 < (4\pi v_R^2 - M_{H_2^0}^2/2), \quad (16)$$

$$M_{H_1^\pm}^2 = \frac{1}{2} (\rho_3 - 2\rho_1) v_R^2 + \frac{1}{4} \alpha_3 \kappa_+^2 < (4\pi v_R^2 - M_{H_2^0}^2/2), \quad (17)$$

$$M_{H_2^\pm}^2 = \frac{1}{2} \alpha_3 v_R^2 + \frac{1}{4} \alpha_3 \kappa_+^2 < 4\pi v_R^2, \quad (18)$$

$$M_{H_1^{\pm\pm}}^2 = \frac{1}{2} (\rho_3 - 2\rho_1) v_R^2 + \frac{1}{2} \alpha_3 \kappa_+^2 < (4\pi v_R^2 - M_{H_2^0}^2/2), \quad (19)$$

$$M_{H_2^{\pm\pm}}^2 = 2\rho_2 v_R^2 + \frac{1}{2} \alpha_3 \kappa_+^2 < 4\sqrt{2}\pi v_R^2. \quad (20)$$

¹ In Eq. (3) VEVs are normalized by $\sqrt{2}$, so $\kappa_+ = 246$ GeV, as in [21,70,71]. In [22, 45] there is no such VEVs normalization, so $\kappa_+ = 174$ GeV, and the mass relation for the SM equivalent Higgs boson H_0^0 in Eq. (11) differs accordingly.

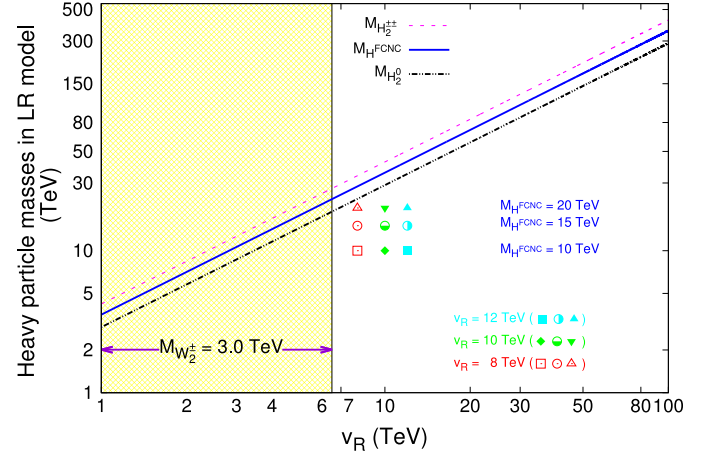


Fig. 1. Upper limits on masses of scalars in MLRSM as a function of v_R . In this plot we define: $M_{H^{\text{FCNC}}} \in [M_{H_1^0}, M_{A_1^0}]$; $M_{H_0^0}$ is the SM Higgs. These limits are outcome of unitarity and vacuum stability constraints discussed in the text. The shaded region of v_R is due to the exclusion limits on W_2^\pm experimental searches, which give typically 3.0 TeV [74] for the restricted MLRSM scenario. Three benchmark points discussed in [43], corresponding to $v_R = 8$ TeV: $M_{H^{\text{FCNC}}} = 10$ (box), 15 (circle), 20 (triangle) TeV are shown. They are compatible with low energy constraints, and also TU and VS constraints for that particular choice of v_R .

In [71] the second term in Eq. (11) has been missed and we sketch its derivation in the Appendix. After the Higgs boson discovery, this mass relation is fixed and can be helpful for RGEs discussion, see Section 5.

4. Vacuum stability criteria

Apart from the TU constraints discussed in the previous section, the quartic couplings have to satisfy necessary conditions for the vacuum stability [69,68]:

$$\lambda_1 \geq 0, \rho_1 \geq 0, \rho_1 + \rho_2 \geq 0, \rho_1 + 2\rho_2 \geq 0. \quad (21)$$

In passing we would like to emphasize few comments on computation of vacuum stability criteria. We have used the vacuum stability criteria computed in [68] using the copositivity conditions, which is an improved version of the positivity idea used in [69]. The copositivity criteria lead to the vacuum stability conditions which encapsulate broader parameter space than that comes from the positivity criteria [69]. Thus, it is indeed possible that for some values of quartic couplings the vacuum looks to be unbounded from below, if we use former criteria. In reality that may not be true, if they satisfy copositivity criteria. Thus, the copositivity criteria as computed in [68] are certainly an improvement over results given in [69]. Here, we would like to mention that one must be careful while computing the copositivity criteria as it has some basis dependency, and for some choices of basis it is possible to encounter some unrealistic stringent criteria.

From Eqs. (5)–(20) it is easy to note that it is not possible to compute the upper limits on the masses of all the scalars individually. This is because for some of the quartic couplings the unitarity constraints are quite entangled and cannot be decoupled. Thus, the upper limits of a few scalar masses are functions of masses of other scalars, e.g., maximum values of $M_{H_3^0}$, $M_{A_2^0}$, $M_{H_1^\pm}$, $M_{H_1^{\pm\pm}}$ depend on $M_{H_2^0}$. So, the unitarity constraints on their masses do not lead to upper limits. Among all the scalars, $H_2^{\pm\pm}$ can be the heaviest for all choices of v_R , see Fig. 1. For $M_{H_1^0}$ and $M_{A_1^0}$ the vacuum stability criteria allows to set the mass upper limits, which would not be possible if we used only unitarity bounds. In Fig. 1 the upper limits on $M_{H_1^0}$, $M_{A_1^0}$ respect the vacuum stability as

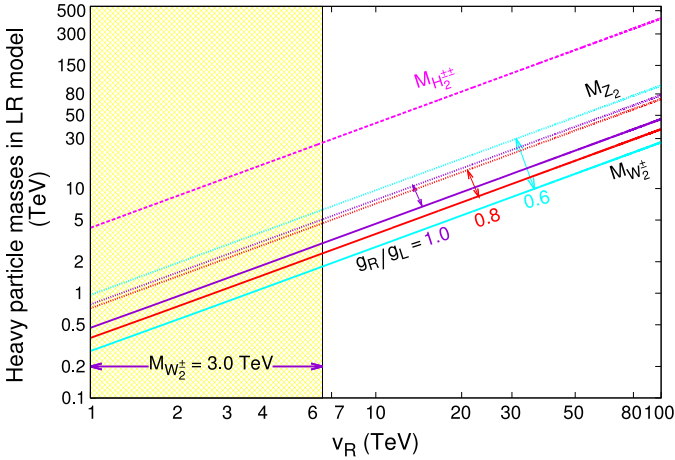


Fig. 2. Masses of heavy gauge bosons in MLRSM scenarios. The mass splittings among W_2^\pm and Z_2 are shown for $g_R/g_L = 1.0, 0.8, 0.6$. The shaded region of v_R is as in Fig. 1. For comparison, the upper limit on $H_2^{\pm\pm}$ from Fig. 1 is included here.

well as unitarity constraints. In Fig. 1 some benchmark points (BP) discussed in [43] are included for readers convenience, the exact spectrum and scalar potential parameters for $v_R = 12$ TeV are repeated in the Appendix. These BPs lead to the degenerate doubly charged Higgs bosons within reach of the LHC and also satisfy VS and FCNC criteria, see Eqs. (9)–(13) in [43]. As we can see, all of them are at the allowed region, though BPs for $M_{\text{HFCNC}} = 20$ TeV marginally (larger masses are disfavoured).

Let us discuss the limit on mass of the gauge boson W_2 related to TU and VS of the scalar potential. We consider the minimal version (MLRSM) of the left-right model where the gauge couplings are equal $g_L = g_R$, and its non-minimal version (MLRSM) where $g_L \neq g_R$. The latter scenario seems to be more suitable if strict gauge coupling unification is assumed [75]. This choice was also discussed in the context of the LHC diboson excesses in [24,27,29,28]. In MLRSM scenario the gauge boson masses are given in an analytical form as [76] ($g_a = g_R/g_L$):

$$M_{W_2}^2 = \frac{g_L^2}{8} \left[(1 + g_a^2)\kappa_+^2 + 2g_a^2 v_R^2 + \sqrt{16g_a^2 \kappa_1^2 \kappa_2^2 + ((g_a^2 - 1)\kappa_+^2 + 2g_a^2 v_R^2)^2} \right], \quad (22)$$

$$M_{Z_2}^2 = \frac{1}{8} \left\{ 4g'^2 v_R^2 + g_L^2 v_R^2 \left[\left(4g_a^2 + \frac{4g'^2}{g_L^2} + \frac{(1 + g_a^2)\kappa_+^2}{v_R^2} \right)^2 - \frac{16(g'^2 + g_a^2(g_L^2 + g'^2))\kappa_+^2}{g_L^2 v_R^2} \right]^{1/2} + g_L^2 (\kappa_+^2 + g_a^2 (\kappa_+^2 + 4v_R^2)) \right\}. \quad (23)$$

g' is the gauge coupling corresponding to $U(1)_{B-L}$ gauge symmetry. In Fig. 2 masses of heavy gauge bosons are given. They depend on gauge couplings and the mass splitting between charged and neutral gauge bosons increases with decreasing g_R/g_L ratio.

This is quite clear if we look at the correlations among the gauge couplings. As g_R decreases one needs larger value of g' to ensure proper value of $U(1)_Y$ gauge coupling, g_Y . That in turn increases M_{Z_2} , and thus the splitting is enlarged. Let us note that naturally $M_{Z_2} > M_{W_2}$, for more exotic scenarios, see [77].

As $\kappa_+ \ll v_R$, mass of W_2 in MLRSM ($g_L = g_R = g_2$) is given by $M_{W_2} = g_2 v_R / \sqrt{2}$. Hence, a limit on M_{W_2} is strictly related to the limit on v_R . The latter, in turn, has to be bigger than

$$v_R \gtrsim \frac{\sqrt{2} M_{\text{HFCNC}}}{\sqrt{\alpha_3}}, \quad (24)$$

in order to ensure that masses of H_1^0 and A_1^0 are greater than $M_{\text{HFCNC}} \approx 10$ TeV. This is the lowest limit on FCNC Higgs bosons [60], one of the strongest limits has been obtained in [78] ($M_{\text{HFCNC}} \geq 50$ TeV). Taking $M_{\text{HFCNC}} \approx 10$ (20, 50) TeV and $\alpha_3 \leq 8\pi$, see Eq. (8), we get

$$M_{W_2} \geq \frac{g_2 M_{\text{HFCNC}}}{\sqrt{8\pi}} \approx 1.3 \text{ (2.6, 6.5) TeV}. \quad (25)$$

This is the lowest limit on the charged gauge boson mass with a minimal theoretical assumption which takes into account scalar sector of the model.

Similar bounds as in Eq. (25) can be obtained for M_{Z_2} , $M_{Z_2} \simeq 1.66 \times M_{W_2}$ in MLRSM.

5. Renormalization group evolution

In the SM, after Higgs boson discovery² there are arguments that at 1-loop and beyond there are no Landau poles up to the Planck mass scale [79]. It is interesting to note that the Higgs self-coupling λ as well as the top-quark Yukawa coupling y_t at one loop are asymptotically free for parameter range fixed by recent data. This is not changed by higher corrections up to three loops. However, if the Higgs self coupling would be bigger, there would be a Landau pole at very high scales, see for instance [80]. For SM the existence of a Landau pole depends mainly on the value of the top-quark Yukawa coupling y_t . Here, the situation is not very transparent. In some analysis, e.g. [81], the Higgs β -function vanishes around 10^9 GeV, whereas according to [79], its zero occurs at about 10^{17} GeV with lower y_t . In this better scenario the Landau pole is appearing but far beyond the Planck scale.

We can see how fragile are the results and conclusions based on renormalization group (RG) analysis in the SM. So, what can we expect within the beyond SM scenario? Here, the higher order corrections are even more complicated. But they can be crucial in some corner of the parameter space: imagine that either λ or y_t are adjusted such that Higgs beta function is positive. Then a Landau pole at some high scale may emerge, and it is quite possible that higher loop corrections can cause the change in sign of beta-functions. In this way the stability analysis can be performed with better accuracy.

Let us discuss RG evolution of the scalar potential parameters. To that end we shall use 1-loop RG equations. As computation of β function coefficients is error prone especially in a model with many couplings in the scalar potential, we have used the PyR@TE (v1.2.2 beta) package [82,83] to automatically generate 1-loop RGEs for MLRSM.

The explicit form of RGEs has already been given e.g. in [67]. Those formulas were latter used, e.g., in [68,69,17]. In this article we have made following progress and improvements in this context:

- We have computed the full set of RGEs. For example the renormalization group evolution of one of the quartic couplings is computed as:

² The Higgs boson mass is not a free parameter any more and RGEs need one less free parameter.

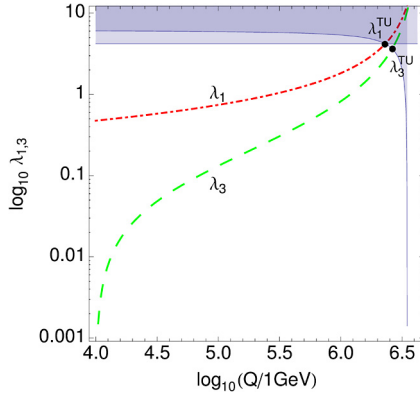


Fig. 3. RG running of $\lambda_{1,3}$ from scale $Q = v_R$ up to $Q \approx 10^{6.5}$ GeV where Landau pole appears. Red dot-dashed line corresponds to $\lambda_1(Q)$ while green dashed line represents $\lambda_3(Q)$. $\lambda_{2,4}(Q) \approx 0$ are not shown on the plot. Shaded region corresponds to the exclusion limits provided by the unitarity bounds (5) and (6) which need to be respected by λ_1 and λ_3 . Black dots with labels $\lambda_{1,3}^{TU}$ show where $\lambda_{1,3}$ enter region forbidden by the Tree-Unitarity. (For interpretation of the references to color in this figure legend, the reader is referred to the web version of this article.)

$$(4\pi)^2 \frac{d\lambda_3}{d \ln Q} = +\frac{64}{3}\lambda_2\lambda_3 - 9g_R^2\lambda_3 + \frac{64}{3}\lambda_2^2 - 9g_L^2\lambda_3 + 32\lambda_3^2 + 24\lambda_1\lambda_3 + \mathcal{O}(\lambda y^2) + \mathcal{O}(y^4).$$

Let us note that there is no term $\propto g^2$ unlike given in [67]. Also a term like $(+\frac{64}{3}\lambda_2\lambda_3)$ was absent in [67].

- We have also provided the evolutions of scalar mass parameters.
- Our RGEs contain right and left handed gauge couplings separately thus can be used for non-minimal models where $g_L \neq g_R$.
- The Yukawa couplings are appearing as matrices so the scenario with non-diagonal Yukawa couplings and their mixing effects can be adjudged. As RGEs of the couplings are coupled, these new and correct set of equations will be very important for future analyses.

Rather than displaying all coupled complicated and clumsy equations, we have included them in related MATHEMATICA file which was automatically generated using PYR@TE. That file LR-RGES-1-loop.m together with numerical routines for solving 1-loop RGEs can be downloaded from [73]. In the Appendix we have encoded only one example of the RGEs to show their structures and complexities.

We will not discuss the evolution of mass parameters μ_i^2 , see (28), as they are not relevant for our analysis. Let us only note that their values at the scale v_R are given by extremization conditions of the scalar potential, see [21,70]. Hence $\mu_i^2(v_R)$ can be expressed with the help of initial values for remaining free parameters of the model i.e. $\alpha_i(v_R)$, $\lambda_j(v_R)$, $\rho_k(v_R)$ and mass scales κ_+ , v_R .

For the simplicity, we assume that $v_R \sim 14$ TeV which is safe as we have noted in our earlier section, and all the masses (12)–(20) are $\mathcal{O}(v_R)$. The only mass which is fixed is the mass of the lightest Higgs boson H_0^0 . It gives relation between values of λ_1 , α_1 and ρ_1 , see (11).

The parameters of the scalar potential which do not explicitly enter formulas (11)–(20) are set to zero at the scale $Q_0 = v_R/\sqrt{2}$:

$$\alpha_2(Q_0) = \lambda_{2,3,4}(Q_0) = \rho_4(Q_0) = 0. \quad (26)$$

It turns out that such values of α_2 , $\lambda_{2,4}$ and ρ_4 are stable under RG evolution. To present typical behaviour of the model under RG flow let us set the values of the remaining parameters at Q_0 as follows:

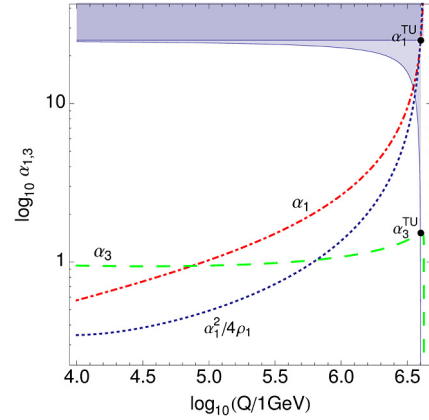


Fig. 4. RG running of $\alpha_{1,3}$ from scale $Q = v_R$ up to $Q \approx 10^{6.5}$ GeV where Landau pole appears. Red dot-dashed line corresponds to $\alpha_1(Q)$ while green dashed line represents $\alpha_3(Q)$. $\alpha_2(Q) \approx 0$ is not shown on the plot. Shaded region corresponds to the exclusion limits provided by the unitarity bounds (8) which must be respected by α_1 and α_3 . Black dots with labels $\alpha_{1,3}^{TU}$ show where $\alpha_{1,3}$ enter region forbidden by the Tree-Unitarity. Blue dotted line displays RG running of the ratio $\alpha_1^2/4\rho_1$ which appears in (11). (For interpretation of the references to color in this figure legend, the reader is referred to the web version of this article.)

$$\frac{1}{2}\alpha_3(Q_0) = 2\rho_{1,2}(Q_0) = \frac{1}{2}[\rho_3(Q_0) - 2\rho_1(Q_0)]$$

$$= \left(\frac{g_2}{\sqrt{2}} \frac{M_{\text{HFCNC}}}{M_{W_2}} \right)^2 \approx 0.48 \quad (27)$$

Such choice results in nearly equal masses of $H_{1,2,3}^0$, $A_{1,2}^0$, $H_{1,2}^\pm$ and $H_{1,2}^{\pm\pm}$ and moreover ensures that $M_{H_1^0} \approx 10$ TeV. The initial value of λ_1 was set to 0.48. It yields a typical behaviour of that parameter under RG evolution, see Fig. 3. It is interesting to note that varying λ_1 in the range $[0.1 - 1.5]$ results in a shift of a position of the Landau pole from 10^7 GeV to 10^5 GeV. Finally, let us recall that due to (11), the value of $\alpha_1(Q_0)$ is also fixed. Hence all the initial conditions are specified. Contrary to [67], where the RGE running of only specific terms of scalar potential couplings were considered, in this work we choose such initial values of scalar potential parameters, see (27), that result in a well-defined mass spectrum. It means that all the scalar masses are positive, all the experimental bounds on scalar particles masses are satisfied, and stability and Tree-Unitarity conditions are fulfilled, see Eqs. (21) and (5)–(10), respectively.

The obtained RG flow of the parameters from the renormalization scale $Q_0 \approx 10^4$ GeV up to higher scales is shown in Figs. 3, 4 and 5. Let us shortly discuss these results. First, the Landau-pole-type behaviour of $\lambda_{1,3}$, $\alpha_{1,3}$ and $\rho_{1,2,3}$ is clearly visible. The reason for this phenomenon are self-couplings of these parameters which dominate positive contributions to their β functions. As a consequence e.g. $\lambda_{1,3}$, and similarly other couplings, start to increase rapidly when the renormalization scale Q approaches $10^{6.5}$ GeV leading to Landau pole at that scale. Moreover at $Q \approx 10^{6.5}$ GeV the perturbative description of MLRSM breaks down due to the violation of the Tree-Unitarity bounds (7)–(10) by all the couplings. As one can see in Figs. 3–5, close to $Q \approx 10^{6.5}$ GeV the running couplings start to enter the regions of values which are forbidden by the Tree-Unitarity, see points in Figs. 3–5 marked by black dots.

If we choose higher values of initial parameters in Eq. (27), e.g. increasing M_{HFCNC} , Landau poles shift in the direction of lower Q values. It means that a region of stability decreases further, below $Q \sim 10^6$ GeV.

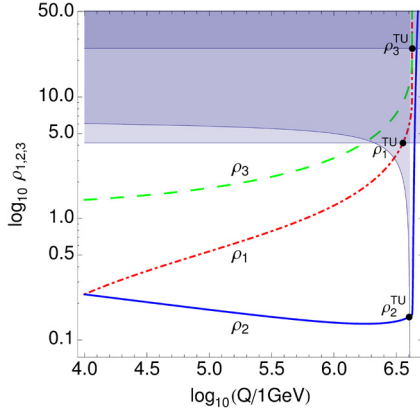


Fig. 5. RG running of $\rho_{1,2,3}$ from scale $Q = v_R$ up to $Q \approx 10^{6.5}$ GeV where Landau pole appears. Red dot-dashed line corresponds to $\rho_1(Q)$, blue solid line represents $\rho_2(Q)$, while green dashed line shows $\rho_3(Q)$. $\rho_4(Q) \approx 0$ is not displayed on the plot. Shaded region corresponds the exclusion limits provided by the unitarity bounds (9) and (10) which need to be respected by ρ_1 , ρ_2 and ρ_3 . Black dots with labels $\rho_{1,2,3}^{\text{TU}}$ show where $\rho_{1,2,3}$ enter region forbidden by the Tree-Unity. (For interpretation of the references to color in this figure legend, the reader is referred to the web version of this article.)

6. Conclusions and outlook

The constraints from Tree-Unity give a good handle to understand the spectrum of the heavy scalar fields within the Left-Right symmetric models. We expressed TU in terms of the physical scalar fields, thus we have been able to translate those constraints into the maximal mass limits of some beyond Standard Model heavy particles. Along with that we impose the vacuum stability criteria to further constrain the parameter space. We have discussed the status of the benchmark points which we suggested in our earlier paper compatible with lack of FCNC effects, and which are interesting in the context of the LHC phenomenological aspects. All these constraints together leave a well defined room in the parameter space, as a function of v_R . In the process we have come up with general and complete set of 1-loop renormalization group equations for all couplings of the considered model. We have performed evolutions of quartic couplings using these complete set of RGEs and shown how large the right-handed scale can be. It appears that restrictions coming from TU and RGEs meet approximately at the same Q scale which is also controlled by the choice of M_{HFCNC} .

One of the possible future directions is to perform the full 2-loop analysis of RG flow of scalar potential parameters taking into account the impact of the threshold corrections and proper matching conditions. They are crucial when one allows large mass splitting among the heavy scalars. And this feature is important for further phenomenological studies. To ensure proper breaking of the electroweak symmetry, a bottom-up approach would be more appropriate for such analysis. Another important fact in this kind of analysis is a possible emergence of Landau poles at relatively low Q scale which signals that the perturbativity can be in trouble. Thus one should perform this computation for higher orders as well with the hope that incorporation of 2-loop corrections may alleviate this problem. In this context the impact of heavy right-handed neutrino Yukawa coupling at the two-loop level cannot be ignored, and their roles have been already noticed at the 1-loop level low-energy muon decay analysis in [41]. Similar to the other fermion loops, the higher order corrections involving heavy neutrinos also contribute negatively to the beta functions of the quartic couplings and thus can delay the disaster of hitting the Landau pole. It is also known that 2-loop contributions to RGEs can signif-

icantly change running especially in the regime where parameters are bigger than 1.

Acknowledgements

JG greatly appreciates the warm hospitality of Dept. of Physics, IIT Kanpur where part of the work was done. We would like to thank Ira Rothstein for comments on RGEs of the MLRSM and Florian Lyonnet for comments and suggestions related to the usage of PyR@TE package. Work supported by Department of Science & Technology, Government of INDIA under the Grant Agreement number IFA12-PH-34 (INSPIRE Faculty Award) and by the Polish National Science Centre (NCN), Grant No. DEC-2013/11/B/ST2/04023.

Appendix A

The full scalar potential includes left and right-handed triplets [21,70,71]:

$$\begin{aligned}
 V(\phi, \Delta_L, \Delta_R) = & \\
 & + \lambda_1 \left\{ \left(\text{Tr}[\phi^\dagger \phi] \right)^2 \right\} + \lambda_2 \left\{ \left(\text{Tr}[\tilde{\phi} \phi^\dagger] \right)^2 + \left(\text{Tr}[\tilde{\phi}^\dagger \phi] \right)^2 \right\} \\
 & + \lambda_3 \left\{ \text{Tr}[\tilde{\phi} \phi^\dagger] \text{Tr}[\tilde{\phi}^\dagger \phi] \right\} \\
 & + \lambda_4 \left\{ \text{Tr}[\phi^\dagger \phi] \left(\text{Tr}[\tilde{\phi} \phi^\dagger] + \text{Tr}[\tilde{\phi}^\dagger \phi] \right) \right\} \\
 & + \rho_1 \left\{ \left(\text{Tr}[\Delta_L \Delta_L^\dagger] \right)^2 + \left(\text{Tr}[\Delta_R \Delta_R^\dagger] \right)^2 \right\} \\
 & + \rho_2 \left\{ \text{Tr}[\Delta_L \Delta_L] \text{Tr}[\Delta_L^\dagger \Delta_L^\dagger] + \text{Tr}[\Delta_R \Delta_R] \text{Tr}[\Delta_R^\dagger \Delta_R^\dagger] \right\} \\
 & + \rho_3 \left\{ \text{Tr}[\Delta_L \Delta_L^\dagger] \text{Tr}[\Delta_R \Delta_R^\dagger] \right\} \\
 & + \rho_4 \left\{ \text{Tr}[\Delta_L \Delta_L] \text{Tr}[\Delta_R^\dagger \Delta_R^\dagger] + \text{Tr}[\Delta_L^\dagger \Delta_L^\dagger] \text{Tr}[\Delta_R \Delta_R] \right\} \\
 & + \alpha_1 \left\{ \text{Tr}[\phi^\dagger \phi] \left(\text{Tr}[\Delta_L \Delta_L^\dagger] + \text{Tr}[\Delta_R \Delta_R^\dagger] \right) \right\} \\
 & + \alpha_2 \left\{ \text{Tr}[\phi \tilde{\phi}^\dagger] \text{Tr}[\Delta_R \Delta_R^\dagger] + \text{Tr}[\phi^\dagger \tilde{\phi}] \text{Tr}[\Delta_L \Delta_L^\dagger] \right\} \\
 & + \alpha_2^* \left\{ \text{Tr}[\phi^\dagger \tilde{\phi}] \text{Tr}[\Delta_R \Delta_R^\dagger] + \text{Tr}[\tilde{\phi}^\dagger \phi] \text{Tr}[\Delta_L \Delta_L^\dagger] \right\} \\
 & + \alpha_3 \left\{ \text{Tr}[\phi \phi^\dagger \Delta_L \Delta_L^\dagger] + \text{Tr}[\phi^\dagger \phi \Delta_R \Delta_R^\dagger] \right\} \\
 & - \mu_1^2 \text{Tr}[\phi^\dagger \phi] - \mu_2^2 (\text{Tr}[\tilde{\phi} \phi^\dagger] + \text{Tr}[\tilde{\phi}^\dagger \phi]) \\
 & - \mu_3^2 (\text{Tr}[\Delta_L \Delta_L^\dagger] + \text{Tr}[\Delta_R \Delta_R^\dagger]). \tag{28}
 \end{aligned}$$

After spontaneous symmetry breaking of the above potential, the mass matrix which includes $M_{H_0^0}$ can be written in the following form (for details, see [21])

$$M = \begin{pmatrix} 2\epsilon^2 \lambda_1 & 2\epsilon^2 \lambda_4 & \alpha_1 \epsilon \\ 2\epsilon^2 \lambda_4 & \frac{1}{2} [4(2\lambda_2 + \lambda_3)\epsilon^2 + \alpha_3] & 2\alpha_2 \epsilon \\ \alpha_1 \epsilon & 2\alpha_2 \epsilon & 2\rho_1 \end{pmatrix}. \tag{29}$$

Expanding eigenvalues of this matrix in a small $\epsilon = \kappa_+/v_R$ parameter Eq. (11) emerges.

The benchmark point considered in the paper resulting in a mass spectrum obtained with the following set of parameters ($v_R = 12$ TeV):

$$\lambda_1 = 0.13, \lambda_2 = 0, \lambda_3 = 0, \lambda_4 = 0, \quad (30)$$

$$\alpha_1 = 0, \alpha_2 = 0, \alpha_3 = 1.39, \quad (31)$$

$$\rho_1 = 1.0, \rho_2 = 7.5 \times 10^{-4}, \rho_3 = 2.003. \quad (32)$$

All masses are given in GeV:

$$M_{H_0^0} = 125, \quad (33)$$

$$M_{H_1^0} = 10000, M_{H_2^0} = 16971, M_{H_3^0} = 465, \quad (34)$$

$$M_{A_1^0} = 10000, M_{A_2^0} = 465, \quad (35)$$

$$M_{H_1^\pm} = 487, M_{H_2^\pm} = 10001, \quad (36)$$

$$M_{H_1^{\pm\pm}} = 508, M_{H_2^{\pm\pm}} = 508. \quad (37)$$

Here, we present an example of 1-loop RGE generated with the help of PyR@TE (v1.2.2 beta) package:

$$(4\pi)^2 \frac{d\lambda_i}{d \ln Q} =$$

$$6\alpha_1^2 + 6\alpha_1\alpha_3 + \frac{5}{2}\alpha_3^2 + \frac{9}{8}g_L^4 + \frac{3}{4}g_L^2g_R^2 + \frac{9}{8}g_R^4$$

$$- 9g_L^2\lambda_1 - 9g_R^2\lambda_1 + 32\lambda_1^2 + 64\lambda_2^2$$

$$+ 16\lambda_1\lambda_3 + 16\lambda_3^2 + 48\lambda_4^2 + 2\lambda_1 \text{Tr}(\tilde{h}_l^\dagger \tilde{h}_l)$$

$$+ 2\lambda_1 \text{Tr}(h_l^\dagger h_l) + 6\lambda_1 \text{Tr}(\tilde{h}_q^\dagger \tilde{h}_q) + 6\lambda_1 \text{Tr}(h_q^\dagger h_q)$$

$$+ 2\lambda_1 \text{Tr}(\tilde{h}_l^* \tilde{h}_l^T) + 2\lambda_1 \text{Tr}(h_l^* h_l^T) + 6\lambda_1 \text{Tr}(\tilde{h}_q^* \tilde{h}_q^T)$$

$$+ 6\lambda_1 \text{Tr}(h_q^* h_q^T) - \text{Tr}(\tilde{h}_l \tilde{h}_l^\dagger \tilde{h}_l \tilde{h}_l^\dagger) - \text{Tr}(h_l h_l^\dagger h_l h_l^\dagger)$$

$$- 3\text{Tr}(\tilde{h}_q \tilde{h}_q^\dagger \tilde{h}_q \tilde{h}_q^\dagger) - 3\text{Tr}(h_q h_q^\dagger h_q h_q^\dagger)$$

$$- \text{Tr}(\tilde{h}_l^T \tilde{h}_l^* \tilde{h}_l^* \tilde{h}_l^T) - \text{Tr}(h_l^T h_l^* h_l^* h_l^T)$$

$$- 3\text{Tr}(\tilde{h}_q^T \tilde{h}_q^* \tilde{h}_q^* \tilde{h}_q^T) - 3\text{Tr}(h_q^T h_q^* h_q^* h_q^T), \quad (38)$$

where h_l, \tilde{h}_l, h_q and \tilde{h}_q are Yukawa couplings, λ_i and α_j are the scalar quartic couplings, g_k are the gauge couplings as defined in Eq. (14) in [71].

References

- [1] G. Aad, et al., Observation of a new particle in the search for the standard model Higgs boson with the ATLAS detector at the LHC, Phys. Lett. B 716 (2012) 1–29.
- [2] S. Chatrchyan, et al., Observation of a new boson at a mass of 125 GeV with the CMS experiment at the LHC, Phys. Lett. B 716 (2012) 30–61.
- [3] J.R. Ellis, M.K. Gaillard, D.V. Nanopoulos, A phenomenological profile of the Higgs boson, Nucl. Phys. B 106 (1976) 292.
- [4] M.J.G. Veltman, Second threshold in weak interactions, Acta Phys. Pol. B 8 (1977) 475.
- [5] S. Weinberg, Mass of the Higgs boson, Phys. Rev. Lett. 36 (1976) 294–296.
- [6] B.W. Lee, C. Quigg, H.B. Thacker, The strength of weak interactions at very high-energies and the Higgs boson mass, Phys. Rev. Lett. 38 (1977) 883–885.
- [7] B.W. Lee, C. Quigg, H.B. Thacker, Weak interactions at very high-energies: the role of the Higgs boson mass, Phys. Rev. D 16 (1977) 1519.
- [8] H. Huffer, G. Pocsik, Unitarity bounds on Higgs boson masses in the Weinberg–Salam model with two Higgs doublets, Z. Phys. C 8 (1981) 13.
- [9] S. Kanemura, T. Kubota, E. Takasugi, Lee–Quigg–Thacker bounds for Higgs boson masses in a two doublet model, Phys. Lett. B 313 (1993) 155–160.
- [10] A.G. Akeroyd, A. Arhrib, E.-M. Naimi, Note on tree level unitarity in the general two Higgs doublet model, Phys. Lett. B 490 (2000) 119–124.
- [11] J. Horejsi, M. Kladiva, Tree-unitarity bounds for THDM Higgs masses revisited, Eur. Phys. J. C 46 (2006) 81–91.
- [12] I. Chakraborty, A. Kundu, Two-Higgs doublet models confront the naturalness problem, Phys. Rev. D 90 (11) (2014) 115017.
- [13] N. Chakraborty, High-scale validity of a model with three-Higgs-doublets, Phys. Rev. D 93 (7) (2016) 075025.
- [14] N. Chakraborty, B. Mukhopadhyaya, High-scale validity of a two Higgs doublet scenario: metastability included, arXiv:1603.05883.
- [15] M. Aoki, S. Kanemura, Unitarity bounds in the Higgs model including triplet fields with custodial symmetry, Phys. Rev. D 77 (9) (2008) 095009.
- [16] P. Dey, A. Kundu, B. Mukhopadhyaya, Some consequences of a Higgs triplet, J. Phys. G 36 (2009) 025002.
- [17] T. Mondal, U.K. Dey, P. Konar, Implications of unitarity and charge breaking minima in a left-right symmetric model, Phys. Rev. D 92 (9) (2015) 096005.
- [18] G. Senjanovic, R.N. Mohapatra, Exact left-right symmetry and spontaneous violation of parity, Phys. Rev. D 12 (1975) 1502.
- [19] R.N. Mohapatra, G. Senjanovic, Neutrino mass and spontaneous parity violation, Phys. Rev. Lett. 44 (1980) 912.
- [20] R.N. Mohapatra, G. Senjanovic, Neutrino masses and mixings in gauge models with spontaneous parity violation, Phys. Rev. D 23 (1981) 165.
- [21] J. Gunion, J. Grifols, A. Mendez, B. Kayser, F.I. Olness, Higgs bosons in left-right symmetric models, Phys. Rev. D 40 (1989) 1546.
- [22] A. Maiezza, M. Nemevsek, F. Nesti, Perturbativity and mass scales of left-right Higgs bosons, arXiv:1603.00360.
- [23] K. Kannike, Vacuum stability of a general scalar potential of a few fields, arXiv:1603.02680.
- [24] F.F. Deppisch, T.E. Gonzalo, S. Patra, N. Sahu, U. Sarkar, Signal of right-handed charged gauge bosons at the LHC?, Phys. Rev. D 90 (5) (2014) 053014.
- [25] F.F. Deppisch, L. Graf, S. Kulkarni, S. Patra, W. Rodejohann, N. Sahu, U. Sarkar, Reconciling the 2 TeV excesses at the LHC in a linear seesaw left-right model, Phys. Rev. D 93 (1) (2016) 013011.
- [26] B.A. Dobrescu, Z. Liu, A W' boson near 2 TeV: predictions for run 2 of the LHC, arXiv:1506.06736.
- [27] J. Gluza, T. Jelinski, Heavy neutrinos and the $pp \rightarrow lljj$ CMS data, Phys. Lett. B 748 (2015) 125–131.
- [28] M. Dhuria, C. Hati, U. Sarkar, Explaining the CMS excesses, baryogenesis and neutrino masses in E_6 motivated $U(1)_N$ model, arXiv:1507.08297.
- [29] J. Brehmer, J. Hewett, J. Kopp, T. Rizzo, J. Tattersall, Symmetry restored in dibosons at the LHC?, arXiv:1507.00013.
- [30] P.S. Bhupal Dev, R.N. Mohapatra, Unified explanation of the $eejj$, diboson and dijet resonances at the LHC, Phys. Rev. Lett. 115 (18) (2015) 181803.
- [31] J. Chakraborty, A. Choudhury, P. Ghosh, S. Mondal, T. Srivastava, Di-photon resonance around 750 GeV: shedding light on the theory underneath, arXiv:1512.05767.
- [32] U.K. Dey, S. Mohanty, G. Tomar, 750 GeV resonance in the dark left-right model, arXiv:1512.07212.
- [33] A. Dasgupta, M. Mitra, D. Borah, Minimal left-right symmetry confronted with the 750 GeV di-photon excess at LHC, arXiv:1512.09202.
- [34] P.S.B. Dev, R.N. Mohapatra, Y. Zhang, Quark seesaw, vectorlike fermions and diphoton excess, J. High Energy Phys. 02 (2016) 186.
- [35] F.F. Deppisch, C. Hati, S. Patra, P. Pritimita, U. Sarkar, Implications of the diphoton excess on left-right models and gauge unification, arXiv:1601.00952.
- [36] D. Borah, S. Patra, S. Sahoo, Subdominant left-right scalar dark matter as origin of the 750 GeV di-photon excess at LHC, arXiv:1601.01828.
- [37] C. Hati, Explaining the diphoton excess in alternative left-right symmetric model, arXiv:1601.02457.
- [38] J. Ren, J.-H. Yu, $SU(2) \times SU(2) \times U(1)$ interpretation on the 750 GeV diphoton excess, arXiv:1602.07708.
- [39] D.T. Huang, P.V. Dong, Left-right asymmetry and 750 GeV diphoton excess, arXiv:1603.05146.
- [40] B.A. Dobrescu, Z. Liu, Heavy Higgs bosons and the 2 TeV W' boson, arXiv:1507.01923.
- [41] J. Chakraborty, J. Gluza, R. Seivillano, R. Szafron, Left-right symmetry at LHC and precise 1-loop low energy data, J. High Energy Phys. 1207 (2012) 038.
- [42] G. Bambhaniya, J. Chakraborty, J. Gluza, M. Kordiaczynska, R. Szafron, Left-right symmetry and the charged Higgs bosons at the LHC, J. High Energy Phys. 05 (2014) 033.
- [43] G. Bambhaniya, J. Chakraborty, J. Gluza, T. Jelinski, M. Kordiaczynska, Lowest limits on the doubly charged Higgs boson masses in the minimal left-right symmetric model, Phys. Rev. D 90 (9) (2014) 095003.
- [44] G. Bambhaniya, J. Chakraborty, J. Gluza, T. Jelinski, R. Szafron, Search for doubly charged Higgs bosons through vector boson fusion at the LHC and beyond, Phys. Rev. D 92 (1) (2015) 015016.
- [45] P.S.B. Dev, R.N. Mohapatra, Y. Zhang, Probing the Higgs sector of the minimal left-right symmetric model at future hadron colliders, arXiv:1602.05947.
- [46] G. Senjanovic, A. Sokorac, Effects of heavy Higgs scalars at low-energies, Phys. Rev. D 18 (1978) 2708.
- [47] J.A. Grifols, Higgs bosons in a left-right symmetric gauge model, Phys. Rev. D 18 (1978) 2704.
- [48] F.I. Olness, M.E. Ebel, Constraints on the Higgs boson masses in left-right electroweak gauge theories, Phys. Rev. D 32 (1985) 1769.
- [49] M. Frank, H. Hamidian, C.S. Kalman, Hadronic decay widths of Higgs bosons in the left-right symmetric model, Phys. Rev. D 45 (1992) 241–246.
- [50] D. Chang, X.-G. He, W.-Y. Keung, B.H.J. McKellar, D. Wyler, Neutron electric dipole moment due to Higgs exchange in left-right symmetric models, Phys. Rev. D 46 (1992) 3876–3883.

- [51] J. Maalampi, A. Pietilae, Higgs contribution to the W pair production in left-right electroweak model, *Z. Phys. C* 59 (1993) 257–262.
- [52] J. Gluza, M. Zralek, Higgs boson contributions to neutrino production in e^-e^+ collisions in a left-right symmetric model, *Phys. Rev. D* 51 (1995) 4695–4706.
- [53] G. Bhattacharyya, A. Raychaudhuri, Constraining the charged Higgs mass in the left-right symmetric model from $b \rightarrow s\gamma$, *Phys. Lett. B* 357 (1995) 119–124.
- [54] G.G. Boyarkina, O.M. Boyarkin, A.N. Senko, Higgs bosons in the left-right model, *Eur. Phys. J. C* 13 (2000) 99–115.
- [55] G. Barenboim, M. Gorbahn, U. Nierste, M. Raidal, Higgs sector of the minimal left-right symmetric model, *Phys. Rev. D* 65 (2002) 095003.
- [56] I. Gogoladze, Y. Mimura, S. Nandi, Gauge Higgs unification on the left right model, *Phys. Lett. B* 560 (2003) 204–213.
- [57] G. Azuelos, K. Benslama, J. Ferland, Prospects for the search for a doubly-charged Higgs in the left-right symmetric model with ATLAS, *J. Phys. G* 32 (2) (2006) 73–91.
- [58] K. Kiers, M. Assis, A.A. Petrov, Higgs sector of the left-right model with explicit CP violation, *Phys. Rev. D* 71 (2005) 115015.
- [59] D.-W. Jung, K.Y. Lee, Production of the charged Higgs bosons at the CERN large hadron collider in the left-right symmetric model, *Phys. Rev. D* 78 (2008) 015022.
- [60] D. Guadagnoli, R.N. Mohapatra, TeV scale left right symmetry and flavor changing neutral Higgs effects, *Phys. Lett. B* 694 (2011) 386–392.
- [61] M. Blanke, A.J. Buras, K. Gemmler, T. Heidsieck, $\Delta F = 2$ observables and $B \rightarrow Xq$ gamma decays in the left-right model: Higgs particles striking back, *J. High Energy Phys.* 03 (2012) 024.
- [62] R.N. Mohapatra, Y. Zhang, LHC accessible second Higgs boson in the left-right model, *Phys. Rev. D* 89 (5) (2014) 055001.
- [63] U. Aydemir, D. Minic, C. Sun, T. Takeuchi, Higgs mass, superconnections, and the TeV-scale left-right symmetric model, *Phys. Rev. D* 91 (2015) 045020.
- [64] A. Maiezza, M. Nemevšek, F. Nesti, Lepton number violation in Higgs decay at LHC, *Phys. Rev. Lett.* 115 (2015) 081802.
- [65] A. Maiezza, M. Nemevsek, Higgs boson(s) in the minimal left-right model, *Acta Phys. Pol. B* 46 (11) (2015) 2317.
- [66] J. Zinn-Justin, Quantum field theory and critical phenomena, *Int. Ser. Monogr. Phys.* 92 (1996) 1–1008.
- [67] I.Z. Rothstein, Renormalization group analysis of the minimal left-right symmetric model, *Nucl. Phys. B* 358 (1991) 181–194.
- [68] J. Chakraborty, P. Konar, T. Mondal, Copositive criteria and boundedness of the scalar potential, *Phys. Rev. D* 89 (9) (2014) 095008.
- [69] J. Chakraborty, P. Konar, T. Mondal, Constraining a class of B-L extended models from vacuum stability and perturbativity, *Phys. Rev. D* 89 (5) (2014) 056014.
- [70] N.G. Deshpande, J.F. Gunion, B. Kayser, F.I. Olness, Left-right symmetric electroweak models with triplet Higgs, *Phys. Rev. D* 44 (1991) 837–858.
- [71] P. Duka, J. Gluza, M. Zralek, Quantization and renormalization of the manifest left-right symmetric model of electroweak interactions, *Ann. Phys.* 280 (2000) 336–408.
- [72] W.J. Marciano, G. Valencia, S. Willenbrock, Renormalization group improved unitarity bounds on the Higgs boson and top quark masses, *Phys. Rev. D* 40 (1989) 1725.
- [73] Available at <https://github.com/jlgluza/LR>.
- [74] V. Khachatryan, et al., Search for heavy neutrinos and W bosons with right-handed couplings in proton-proton collisions at $\sqrt{s} = 8$ TeV, *Eur. Phys. J. C* 74 (11) (2014) 3149.
- [75] J. Chakraborty, A. Raychaudhuri, GUTs with dim-5 interactions: gauge unification and intermediate scales, *Phys. Rev. D* 81 (2010) 055004.
- [76] T. Jelinski, M. Kordiaczynska, Heavy neutrino masses and mixings at the LHC, *Acta Phys. Pol. B* 46 (11) (2015) 2193.
- [77] S. Patra, F.S. Queiroz, W. Rodejohann, Stringent dilepton bounds on left-right models using LHC data, *Phys. Lett. B* 752 (2016) 186–190.
- [78] M. Pospelov, FCNC in left-right symmetric theories and constraints on the right-handed scale, *Phys. Rev. D* 56 (1997) 259–264.
- [79] F. Jegerlehner, The standard model as a low-energy effective theory: what is triggering the Higgs mechanism?, arXiv:1304.7813.
- [80] T. Hambye, K. Riessellmann, Matching conditions and Higgs mass upper bounds revisited, *Phys. Rev. D* 55 (1997) 7255–7262.
- [81] D. Buttazzo, G. Degrandi, P.P. Giardino, G.F. Giudice, F. Sala, et al., Investigating the near-criticality of the Higgs boson, *J. High Energy Phys.* 1312 (2013) 089.
- [82] F. Lyonnet, I. Schienbein, F. Staub, A. Wingarter, PyR@TE: renormalization group equations for general gauge theories, *Comput. Phys. Commun.* 185 (2014) 1130–1152.
- [83] F. Lyonnet, Automation of non-SUSY two-loop RGEs with PyR@TE: latest developments, arXiv:1510.08841.